

## Weather Radar Interlaced Scanning Strategy

STEVEN V. VASILOFF, RICHARD J. DOVIAK, AND MICHAEL T. ISTOK\*

*National Severe Storms Laboratory, NOAA, Norman, OK 73069*

9 May 1986 and 12 September 1986

### ABSTRACT

The Next Generation Weather Radar (NEXRAD) may use a 5-min volume scan to monitor thunderstorms and provide hazard warnings. Short-lifetime, low-altitude wind shear near airports is a hazard to safe flights that deserves special attention. An interlaced scanning strategy is examined for its effects on the accuracy and reliability of some NEXRAD storm analysis and tracking algorithms that require noninterlaced data. By increasing the elevation step to twice its normal value and starting every other scan at the second step of the corresponding 5-min sequence, a pair of 2½-min sequences is achieved. These can be recombined for use in the NEXRAD algorithms while providing a shorter period between observations of rapidly developing phenomena such as low-altitude wind shear. It is found that differences between storm cell attributes derived from successive noninterlaced scans are about the same as differences between values obtained from interlaced and noninterlaced volume scans for the same time period. Thus, interlaced scanning may halve the wind shear warning time to be provided by the proposed NEXRAD noninterlaced scan strategy without significantly compromising the evaluation of storm attributes. Growth rates of reflectivity and updraft speed for several cells during the growth stage of a severe thunderstorm have been assessed in relation to the need for 2½-min updates to resolve severe thunderstorm phenomena. Results indicate that the growth rates are not so rapid as to require interlaced scanning for this purpose.

### 1. Introduction

The Next Generation Weather Radar (NEXRAD) system is currently under development and will replace the present network of National Weather Service (NWS) and Air Weather Service (AWS) radars. The new radars will be 10 cm wavelength Doppler radars and will thus be able to detect the radial component of winds inside thunderstorms. Of particular interest to the Federal Aviation Administration (FAA), among others, are low-altitude hazardous wind phenomena such as wind shear, which can endanger aircraft safety during approach and departure at airports. Heavy rainfall and hail may also pose a threat to aircraft safety (e.g., Dietenberger, 1985). Mahapatra et al. (1983) provide an excellent overview of hazardous weather at airports.

Probably the most frequent cause of air traffic weather-related mishaps near airports is the downburst (Fujita, 1981)—a strong downdraft usually associated with a thunderstorm. The typical horizontal dimension of a downburst on the high plains is 1 to 3 km; the typical lifetime is 5 to 15 minutes, with a 2–4 min period of severe wind shear (McCarthy and Serafin, 1984). Downbursts in springtime Oklahoma thunderstorms are typically larger scale (4–10 km) than the

high plains downbursts (Eilts, 1985). Because of the short lifetime of downbursts and severe wind shear, there is concern that the proposed NEXRAD 5-min volume scan update rate may be too long for the hazard to be reliably detected and the information to be relayed with enough lead time for an aircraft pilot to take corrective action.

An interlaced scanning strategy (see e.g., Mahapatra and Zrnić, 1984) has been proposed whereby successive volume scans would have a frequency of 2½ min instead of 5 min. Thus, the probability of detecting rapidly developing hazards such as strong downbursts would be increased. We analyze the interlaced strategy two different ways. Section 2 describes the interlaced scanning strategy and its effects on planned storm tracking algorithms that will be used to analyze Doppler radar data in real-time. Section 3 describes growth rates of updraft and reflectivity for several cells during the growth stage of a severe thunderstorm. Figures showing growth rates are shown for only one cell; figures for three others can be seen in Vasiloff et al., 1984. The results are then used to assess the necessity for the interlaced scanning strategy to resolve the development of severe thunderstorms in Oklahoma.

### 2. Effects of interlaced scans on real-time algorithms

The computer algorithms that will be used in real-time by NEXRAD were developed by the Air Force

\* Current affiliation: Sperry Corporation Computer Systems, Treviso, PA 19047.

Geophysics Laboratory (AFGL). These algorithms locate storm cells based upon their 30 dBZ radar reflectivity envelope. A minimum horizontal scale of 4 km is required before a 30 dBZ envelope is identified as a cell. In addition, a cell must be identified on at least two successive elevation-angle steps in order to be tracked. Storm cells meeting these criteria are then described by 11 attributes. The effects of interlaced scans on the accuracy and reliability of these NEXRAD algorithms were determined by comparing algorithm performance on data collected in interlaced vs non-interlaced (contiguous) scan sequences. A scan sequence or volume scan is one in which the radar beam sweeps between two azimuth limits (these could be  $0^\circ$  and  $360^\circ$  if a full azimuthal circle is scanned) while increasing its elevation angle between  $\sim 0^\circ$  and one that tops the storm. Because Doppler radar antennas at the National Severe Storms Laboratory (NSSL) cannot rotate as rapidly as the proposed NEXRAD radar antennas, and in order to compare results obtained from interlaced scans with results from contiguous scans, data used in this study were collected over nar-

row sectors so that each volume was scanned at twice the proposed NEXRAD rate. Thus, sectorized volume scans have a frequency of  $2\frac{1}{2}$  min. Alternate constant-elevation scans are deleted from pairs of volume scans and then recombined to simulate pairs of interlaced volume scans that would take 5 min to acquire (Fig. 1). In the volume of interlaced scans, data collected during scans 1, 3, 5, etc., are separated by  $2\frac{1}{2}$  min from data collected during scans 2, 4, 6, etc., respectively, whereas, in the proposed NEXRAD data collection procedure, corresponding constant-elevation scans are separated by 5 min. Note that the vertical spatial resolution of each of the interlaced volume scans is half that of the contiguous volume scans.

The data used in this part of the study were collected on 20 May 1982. Cell attribute values for a pair of simulated interlaced scan sequences during the period 1802–1807 (all times are CST with seconds omitted; all heights are AGL) are shown in Table 1. Additional data are presented in Vasiloff et al., 1984. The column of data for the period 1802–1805 is from one of the two contiguous scan sequences used to generate the

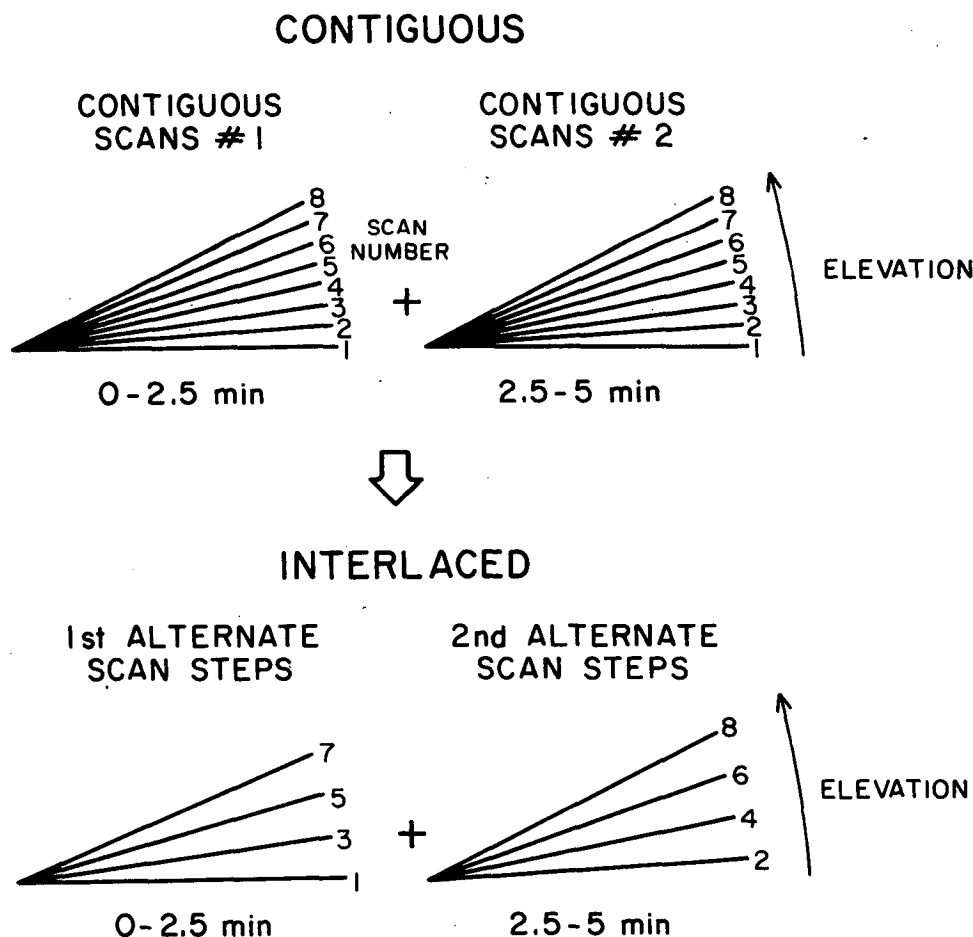


FIG. 1. Simulation of interlaced volume scans by deletion of alternate constant-elevation scans from the contiguous set of volume scans.

TABLE 1. Storm cell attribute values, and differences between them, for noninterlaced (N) and contiguous (I) scanning strategies. Second half of the contiguous scan pair for 1802–1807 is not shown. Seconds have been dropped from the times.

| Attribute*                            | Time (CST)       |                  |                  |                  |                    |
|---------------------------------------|------------------|------------------|------------------|------------------|--------------------|
|                                       | 1757–1801<br>(C) | 1802–1805<br>(C) | 1802–1807<br>(I) | 1807–1810<br>(C) | 1802–1807<br>(C-I) |
| AZM (deg)                             | 248              | 247              | 246              | 249              | 1                  |
| RANGE (km)                            | 103.8            | 98.2             | 98.2             | 88.9             | 0                  |
| HT (km)                               | 5.2              | 5.5              | 5.3              | 4                | 0.2                |
| BASE (km)                             | —                | 2.4              | 2.3              | —                | 0.1                |
| TOP (km)                              | 12.5             | 13.3             | 12.9             | 8.3              | 0.4                |
| MXREF (dBZ)                           | 66               | 67               | 68               | 65               | -1                 |
| ALT (km)                              | 6                | 5.3              | 5.3              | 2.3              | 0                  |
| VOL ( $\times 10^2$ km <sup>3</sup> ) | 37               | 43               | 46               | 69               | -3                 |
| MASS ( $\times 10^5$ kg)              | 42               | 51               | 53               | 73               | -2                 |
| SPEED (m s <sup>-1</sup> )            | 2.9              | 4.9              | 6                | 8                | -1.1               |
| DIR (deg)                             | 294              | 274              | 271              | 258              | 3                  |

\* AZM, RANGE and HT—The 30-dBZ centroid location with respect to the radar. BASE and TOP—The bottom and top of the 30-dBZ contour.

MXREF—The maximum reflectivity factor found in the storm volume (VOL).

ALT—The altitude at which MXREF was found.

VOL—The volume of the storm containing a reflectivity factor of 30 dBZ and greater.

MASS—Mass of the storm within the storm volume (VOL).

SPEED and DIR—The observed motion of the 30-dBZ contour centroid.

interlaced scan sequence. Additional contiguous data are shown for two other time periods as well. The last column lists the differences between attribute values obtained from contiguous and interlaced scans for the time period 1802–1807. It is clear that the differences between attribute values obtained using interlaced data and those obtained using contiguous data are within the uncertainty and variance that generally is seen in attribute values from volume scan to volume scan when contiguous data alone are used. For example, the speed of storm motion derived from contiguous data changes from 2.9 to 4.9 and then to 8.0 m s<sup>-1</sup> over three 5-min periods, whereas only 1.1 m s<sup>-1</sup> difference is found when the storm speed derived from interlaced data is compared with the speed derived from contiguous data collected during the same period. Data collected at other times produce similar results. The most complex algorithm (not shown in table) is the weighted seven-variable test for the likelihood of hail. Both contiguous and interlaced data showed evidence of hail.

### 3. Growth rates of reflectivity and updrafts

Reflectivity and updraft growth rates have been examined for cells of a storm that evolved from a group of small cells into a supercell thunderstorm (Vasiloff et al., 1986). The storm formed in central Oklahoma on 19 June 1980. The National Weather Service Forecast Office in Oklahoma City issued both severe thunderstorm and tornado warnings. The storm was observed with Doppler radars for nearly 2½ h, and 21 dual-Doppler volume scans were obtained. Reference times for analysis begin at 1942 and end at 2215. The median interval between reference times is ~5 min.

Growth rates of reflectivity factor and updraft speed were determined for four cells within the storm at various times. Figures are shown for only one cell; figures for three others can be seen in Vasiloff et al. (1984). A cell is defined as a volume of space that has a reflectivity maximum and an updraft, both of which can be identified in consecutive volume scans. Average cell velocity was from 255° at 9.2 m s<sup>-1</sup>. Each cell formed on the right flank of the storm, moved through the storm, and dissipated on its left flank, giving the storm a motion from 320° at 8.0 m s<sup>-1</sup>, 65° to the right of cell motion.

Figure 2 shows the evolution of peak updraft speed and maximum reflectivity factor at each height in cell C<sub>2</sub>. (The subscript means that C<sub>2</sub> was the second cell to form in the storm complex during the lifetime of the storm.) The diagrams were constructed by plotting maximum values at each level (height separation  $\Delta z = 1$  km) in the cell vs time. The cell first appeared between 6 and 10 km elevation at ~1942. Peak updraft speeds (>25 m s<sup>-1</sup>) occurred about 7 min before the maximum height of the cell (~13 km), and about 20 min before maximum reflectivity factor (50 dBZ). The entire life cycle of C<sub>2</sub> was completed in about 1 h. The maximum reflectivity factor growth rate was ~4 dBZ min<sup>-1</sup> at low and middle altitudes, and the maximum updraft growth rate was ~5 m s<sup>-1</sup> min<sup>-1</sup> at middle to high altitudes.

Reflectivity factor growth rates calculated for the three cells not shown ranged from 4 to 7 dBZ min<sup>-1</sup>. Maximum reflectivity factors ranged from 50 to >60 dBZ, and maximum cell heights ranged from 12 to >16 km. Updraft growth rates ranged from 3 to 7 m s<sup>-1</sup> min<sup>-1</sup>. Peak updraft speeds ranged from 15 to >60 m s<sup>-1</sup>.

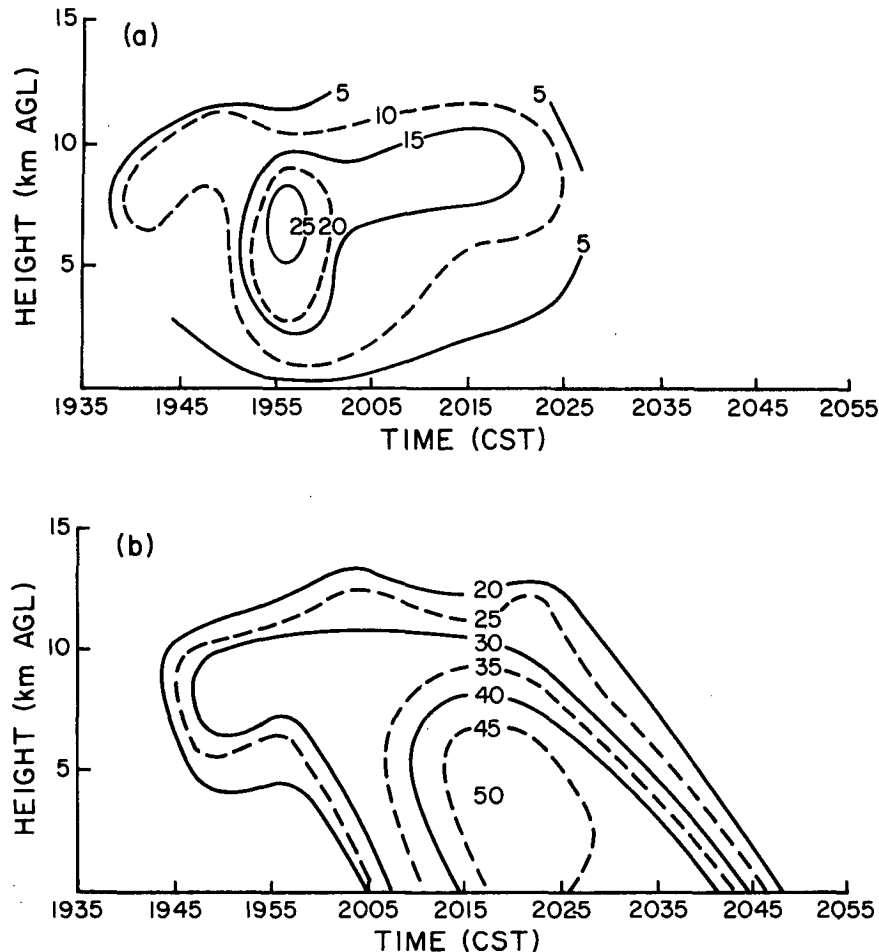


FIG. 2. Evolution of (a) maximum updraft speed ( $\text{m s}^{-1}$ ) and (b) maximum reflectivity factor (dBZ) at each altitude for cell  $C_2$ .

Each cell became more intense than its predecessor while exhibiting similar evolutionary characteristics; peak updrafts occurred  $\sim 10$  min before maximum cell height and as much as 10–20 min before maximum reflectivity. There seemed to be no correlation between high reflectivity and rapid updraft growth rates. However, peak updraft speeds, maximum cell heights and maximum reflectivity appeared to be highly correlated in space, although staggered in time. The cells typically lasted 40 min to 1 h.

Vasiloff et al. (1986) discuss the storm's evolution into a supercell storm where the identification of individual cells and updrafts was very difficult. However, data from 2153 and 2215 showed that peak updraft speeds were consistently  $>45 \text{ m s}^{-1}$  (often exceeding  $60 \text{ m s}^{-1}$ ) and maximum reflectivity factors were  $>60 \text{ dBZ}$ .

#### 4. Summary and discussion

Differences between storm cell attribute values derived from interlaced and contiguous scan sequences

are about the same as differences between attribute values derived from consecutive contiguous scan sequences. Thus, it appears that the proposed interlaced scanning to detect low-altitude wind shear hazards in one-half the time of the proposed NEXRAD contiguous scanning strategy will not have detrimental effects on other algorithms.

However, these results are not entirely conclusive because of variability in algorithm output (especially in determining storm motion) and because the database is inadequate for a thorough statistical examination. In addition, the necessity for obtaining data using interlaced scan sequences cannot be substantiated by the results from the growth rate study described in section 3. For example, a reflectivity growth rate of  $7 \text{ dBZ min}^{-1}$  (maximum found in this study) indicates that a storm with a 65-dBZ peak reflectivity factor would be detected over two 5-min volume scans. Nonetheless, since some important hazardous features such as downbursts occur very rapidly near the surface, their timely detection may indeed necessitate  $2\frac{1}{2}$ -min interlaced scan sequences.

*Acknowledgments.* We would like to thank Msrs. Jean Lee, Don Burgess and Rodger Brown for their critical review, Ms. Joan Kimpel and Mr. Robert Goldsmith who performed the graphics, and Ms. Sandy McPherson and Ms. Michelle Foster who typed the manuscript. Support from the FAA was provided through Contract DTFA01-80-Y-10524.

## REFERENCES

- Dietengberger, M. A., P. A. Haines and J. K. Luers, 1985: Reconstruction of Pan Am New Orleans Accident. *J. Aircraft*, **22**, 719-728.
- Eilts, M. D., and R. J. Doviak, 1986: Oklahoma downbursts and their asymmetry. *J. Climate Appl. Meteor.* in press.
- Fujita, T. T., 1981: Tornadoes and downbursts in the context of generalized planetary scales. *J. Atmos. Sci.*, **38**, 1511-1534.
- Mahapatra, P. R., and D. S. Zrnic', 1984: A physical basis for NEXRAD data update rates. *J. Aircraft*, **21**, 840-850.
- , ——— and R. J. Doviak, 1983: Optimum siting of NEXRAD to detect hazardous weather at airports. *J. Aircraft*, **20**, 363-371.
- McCarthy, J., and R. Serafin, 1984: The microburst: hazard to aviation. *Weatherwise*, **37**, 120-127.
- Ray, P. S., and K. L. Sangren, 1983: Multiple-Doppler radar network design. *J. Climate Appl. Meteor.*, **22**, 1444-1454.
- , C. L. Ziegler, W. Bumgarner and R. J. Serafin, 1980: Single- and multiple-Doppler radar observations of tornadic storms. *Mon. Wea. Rev.*, **108**, 1607-1625.
- Vasiloff, S. V., M. Istok and R. J. Doviak, 1984: Thunderstorm phenomena and weather radar scanning strategies. DOT/FAA/PM-85-14, Final Report, 13 pp.
- , E. A. Brandes, R. P. Davies-Jones and P. S. Ray, 1986: An investigation of the transition from multicell to supercell storms. *J. Climate Appl. Meteor.*, **25**, 1022-1036.